Article

A Deep Learning-Based Method to Detect Hot-Spots in the Visible Video Diagnostics of Wendelstein 7-X

Máté Szűcs [1,*] **, Tamás Szepesi** [1] **, Christoph Biedermann** [2] **, Gábor Cseh** [1] **, Marcin Jakubowski** [2] **, Gábor Kocsis** [1] **, Ralf König** [2] **, Marco Krause** [2] **, Aleix Puig Sitjes** [2] **and the W7-X Team** [†]

[1] Centre for Energy Research, 1121 Budapest, Hungary
[2] Max-Planck-Institute for Plasma Physics, 17491 Greifswald, Germany
[*] Correspondence: szucs.mate@ek-cer.hu
[†] Collaborators/Membership of the W7-X Team is provided in the Acknowledgments.

Abstract: Wendelstein 7-X (W7-X) is currently the largest optimized stellarator in operation in the world. Its main objective is to demonstrate long pulse operation and to investigate the suitability of this type of fusion device for a power plant. Maintaining the safety of the first wall is critical to achieving the desired discharge times of approximately 30 min while keeping a steady-state condition. We present a deep learning-based solution to detect the unexpected plasma-wall and plasma-object interactions, so-called hot-spots, in the images of the Event Detection Intelligent Camera (EDICAM) system. These events can pose a serious threat to the safety of the first wall, therefore, to the operation of the device. We show that sufficiently training a neural network with relatively small amounts of data is possible using our approach of mixing the experimental dataset with new images containing so-called synthetic hot-spots generated by us. Diversifying the dataset with synthetic hot-spots increases performance and can make up for the lack of data. The best performing YOLOv5 Small model processes images in 168 ms on average during inference, making it a good candidate for real-time operation. To our knowledge, we are the first ones to be able to detect events in the visible spectrum in stellarators with high accuracy, using neural networks trained on small amounts of data while achieving near-real-time inference times.

Keywords: first wall protection; video diagnostics; deep learning

1. Introduction

Stellarator-type fusion devices are currently one of the most investigated machines behind tokamaks. Their popularity comes from two main core advantages. First, the lack of induced plasma current makes it possible not to have devastating instabilities, such as disruptions in tokamaks. Secondly, since there is no need for a central solenoid to drive plasma current, a pulsed operation can be omitted, and long pulse steady-state operation of hours is theoretically possible. The experimental investigations of stellarators were slower than those of tokamaks because the complicated magnetic field structures introduced new, previously unknown instabilities. Today, with the help of computer-aided calculations, we can optimize these magnetic fields and create configurations with significantly reduced instabilities.

Wendelstein 7-X (W7-X) in Greifswald, Germany, is currently the largest of such optimized stellarators in operation in the world. Its main objective is to demonstrate long pulse operation and to investigate the suitability of this type of fusion device for a power plant. [1–5] Even with the lack of the previously mentioned current-induced instabilities, there are several dangerous phenomena which can harm the first wall of the device and put the steady-state operation at risk. The monitoring of these unexpected plasma-wall/object interactions (hot-spots) is crucial and is done by multiple diagnostics on W7-X. [6] Examples of these so-called "hot-spots" can be seen in Figure 1.
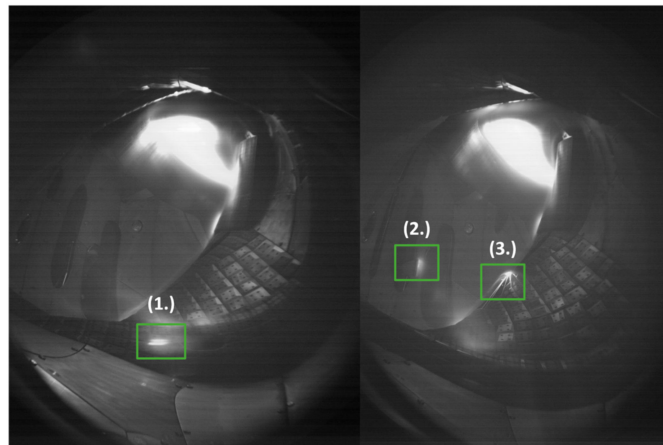
Figure 1. Three examples of hot-spots detected in the images of the visible video diagnostics. (**1.**) A hot-spot on the shielding of the magnetic diagnostics, created by the misconfiguration of the magnetic field structure. (**2.**) A hot-spot on the reciprocating probe. (**3.**) A hot-spot made from debris falling into the vessel.

Machine- and deep-learning methods are gaining popularity in nuclear fusion thanks to their ability to solve complex tasks if sufficient amounts of data are available. We have seen applications ranging from controlling tokamak plasmas [7] and acting as surrogate models [8,9] to enhancing diagnostics [10–12]. Our contribution to this emerging field in nuclear fusion is described in this paper. To our knowledge, we are the first ones to be able to detect events in the visible spectrum in stellarators with high accuracy, using neural networks trained on small amounts of data while achieving near-real-time inference times.

The rest of the paper is structured and organized as follows. In Section 2, we discuss one of the diagnostics used to ensure the safety of the first wall, namely the visible video diagnostics. In Section 3, a deep learning-based method is presented to accurately detect the so-called hot-spots in the images of the visible video diagnostics. In Section 4, the training details and the results are shown. Finally, we conclude our findings and give an outlook in Section 5.

2. Visible Video Diagnostics on W7-X

The video diagnostics on the Wendelstein 7-X stellarator are composed of infrared and visible cameras. Infrared cameras are positioned to monitor the heat loads on the island divertors directly and can signal if the heat loads exceed a threshold. The visible cameras are multipurpose in the sense that while they are crucial for monitoring the first wall of the device, several other plasma phenomena can be observed by them, too—for example, turbulence, plasma filaments, detachment, and other plasma size variations [13].

As seen in Figure 2., the visible cameras are located in ten toroidally viewing "AEQ" ports. This setup enables us to cover approximately 95% of the first wall. Because of the harsh environment and the complicated access to the vessel, the camera heads are found at the end of 2 m long flexible tubes. Containing only the most important electronics and optics, the head is connected to an outer image processing and control unit via a fiber link. In most of the ports, an Event Detection Intelligent Camera (EDICAMs) [14] is installed. The EDICAMs were designed for fusion plasma physics applications. They use a 1.3-megapixel CMOS sensor, which can work perfectly even at strong magnetic fields and moderate radiation levels. The sensors offer non-destructive readout capabilities, which enable the simultaneous monitoring of the whole 1280 × 1024 frame and smaller regions of interest (ROIs) with a faster framerate.
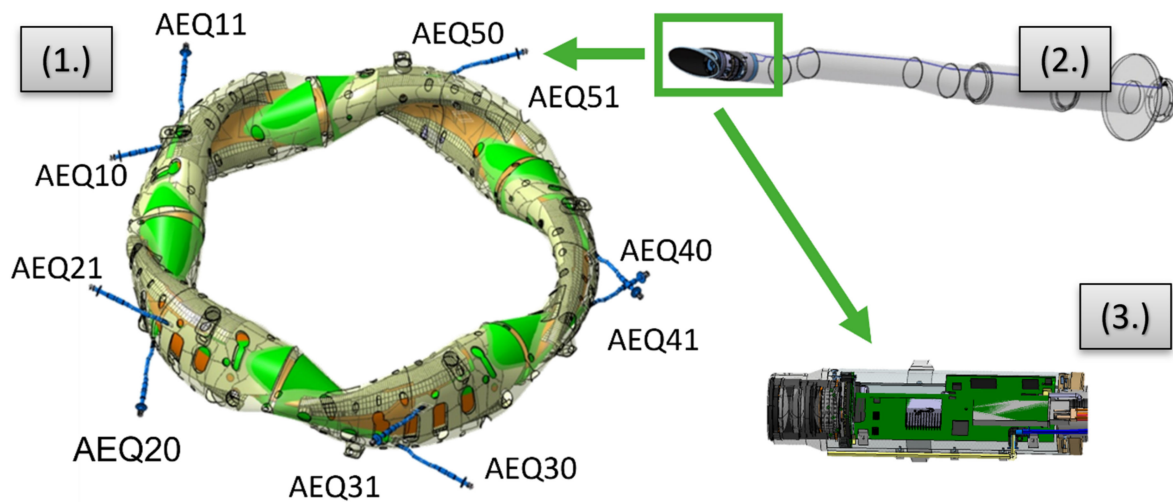
Figure 2. (**1**.) Overview of the visible video diagnostics ports in the vessel. (**2**.) One of the AEQ ports is connected with a flexible tube. (**3**.) A camera head containing only the most important electronics and optics.

3. Real and Synthetic Hot-Spots

Our task at hand was to find a method using which we can accurately detect hot-spots in the images of the EDICAMs at near-real-time speeds. Object detection tasks usually utilize classical image processing algorithms, like applying several filtering methods after thresholding the greyscale image. One such application in nuclear fusion can be found in [15], where the authors used thresholding and centroid identification to detect MARFEs in the JET tokamak. These methods were explored by us but did not bring sufficient results. Thresholding with fixed or adaptive values proved to be too difficult due to several non-hot-spot visibly radiating phenomena being present in the images. The divertor area emits light most of the time and could be masked out from the images to then apply the algorithms, but the radiating mantle of the plasma in the edge was still too distracting and tricked the algorithms too easily. The radiating mantle (or radiation belt) is seen in images both from tokamaks and stellarators. It is the visible radiation from the plasma edge. The main difference between its presence in these two machines is that stellarators can vary in size, shape, location, and intensity. The irregular shapes are caused by the "exotic" 3D geometry of the magnetic field lacking real symmetries. Because of this, our cameras see the superposition of poloidal cross-sections at different toroidal locations. Its overall intensity depends on the heating power but is usually evenly distributed, so it could be removed with top-hat transformation. However, in some cases, the radiation belt can largely differ from its "normal" shape and location, these cases being some different magnetic configurations and diverter or plasma detachment. The top-hat transformation, given these changes, frequently left artifacts in the images which would later be falsely classified as hot-spots. As a result of these observations, we chose to use neural network-based object detection models.

We used the YOLOv5 open-source architecture's two smallest versions, namely: YOLOv5 Nano and YOLOv5 Small [16]. We were limited both by the amounts of data and computing power available; thus, these two models seemed to be the right choices. While we had several occurrences of hot-spots during the previous experimental campaigns of W7-X, these images do not necessarily count as multiple data for training our models. Most of the hot-spots appeared at the same locations and usually did not change drastically in shape or in intensity, even when being present for several discharges. Still, training neural networks require considerable amounts of data, so we came up with the idea of generating synthetic hot-spots. We expected that mixing these synthetically generated data with real images from the experiments would allow us to train better-performing models.

The process of creating images with synthetic hot-spots is shown in Figure 3. First, we randomly drop points into a 2D plane and connect them with a bounding contour, which is then painted white against a black background. Secondly, we apply Gauss-filtering to the so-called "blobs" acquired with random sigmas sampled from a given range. Finally, the blobs are superimposed on background images containing no hot-spots in random places, with random sizes and intensities.
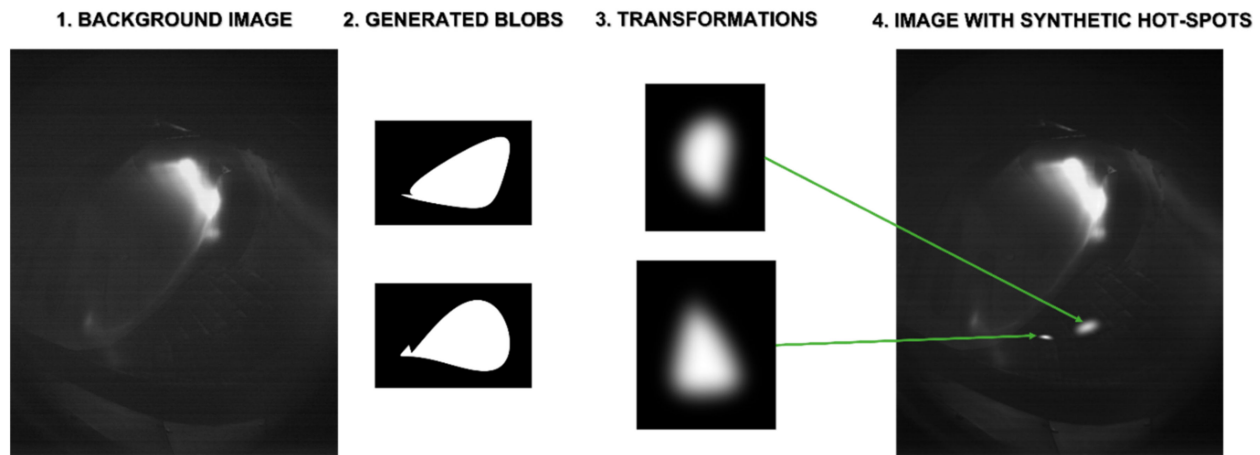

Figure 3. The steps in the process of generating images with synthetic hot-spots.

4. Training Details and Results

As discussed earlier, training neural networks require large amounts of labeled data. The labeling of such datasets is time-consuming, and the location of hot-spots does not necessarily vary much, making the models less able to generalize to unseen events. Creating additional images with synthetic hot-spots can lead to large amounts of diverse hot-spot data. Such a dataset can even be used at the beginning of a device's life circle when little to less experimental data is available.

Our investigations were twofold: we wanted to see which model performs better trained on a relatively small dataset and whether we could obtain better performance if we mixed the training dataset with images containing synthetic hot-spots. In theory, the YOLOv5 Small model should outperform the other model since it has 7.2 million trainable parameters against the Nano's 1.9 million. However, more trainable parameters usually require more data. We created two training datasets: one contained 471 images, all real experimental data, and in the other one, we added 250 additional synthetic hot-spot images. We did not start the training from scratch. Transfer learning was used, which means that the models were first trained on the so-called ImageNet dataset with approximately 14 million images for detecting everyday objects like planes, glasses, and dogs. The weights of these models were uploaded to GitHub and are kindly made open source by the developers. During transfer learning, we keep the weights of the first ("shallow") layers fixed and only retrained the deeper ones for our problem. The shallow layers usually represent low-level information, and the last ones contain task-specific information. When using transfer learning with pre-trained models, computing time and data needed can be significantly reduced.

All the models were trained for 30 iterations using the recommended training parameters found on the YOLOv5 GitHub page. After training, the models were evaluated on 74 never seen real experimental images as validation data. The performance of the models and datasets can be seen in Figure 4.
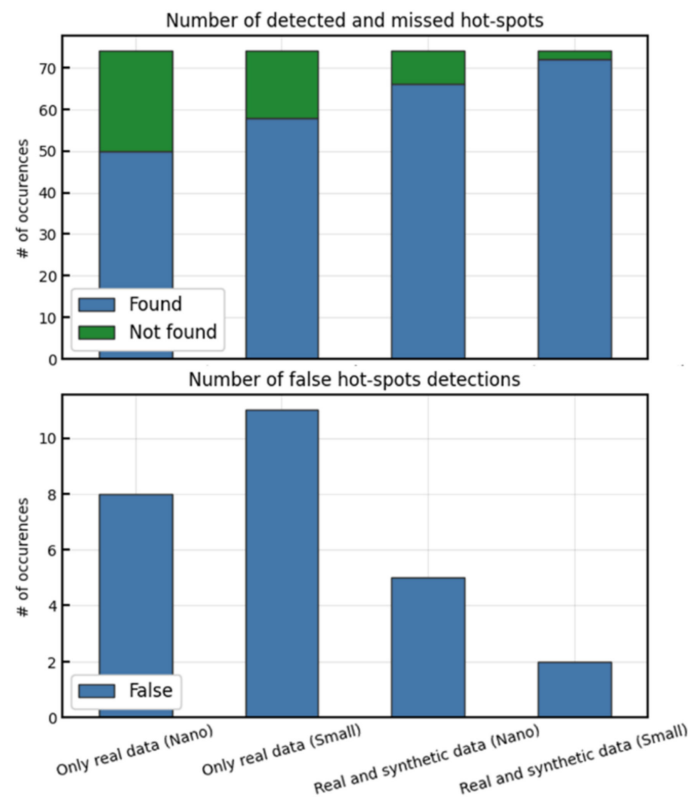
Figure 4. Performance of the models on the 74 never seen real images in the four investigated scenarios.

It can be observed that the larger model outperforms the smaller one in terms of finding real hot-spots even when only trained on 471 images; hence, it is possible to train these models on small datasets thanks to transfer learning. We can also notice that mixing the training dataset with synthetic hot-spots images results in better models in both cases. This reinforces our method of creating synthetic hot-spots. Overall the YOLOv5 Small model trained on the mixed dataset was the best in accurately detecting hot-spots. If we look at the second chart in Figure 4, we can observe the number of false hot-spot detections. While accurately detecting hot-spots is our main priority, we want to keep false alarms at the lowest possible so that we will not interrupt the machine's operation unnecessarily. The fact that using larger models is not always the best option when lacking a sufficient amount of data culminates here. The Small model performs worse than the Nano one when only trained on the 471 real images. However, when we add the synthetic data, this difference is reversed, while all two outperform the previous ones. The runtime of both models during inference was measured in preparation for real-time operation. The Nano architecture processes one image in 75 ms on average, and the Small does it in 168 ms. Both models are good candidates for near-real-time operation in the future.

5. Conclusions

In this paper, a deep learning-based method was presented to accurately detect unexpected plasma-wall/object interactions in the images of the visible video diagnostics of W7-X. We showed that the YOLOv5 object detection models, specifically the smallest Nano and Small models, can achieve high accuracy, even when trained using relatively small amounts of experimental data, if we mix the data with images containing synthetic hot-spots. Diversifying the dataset with synthetic hot-spots increases performance and can make up for the lack of data. A simple algorithm for a synthetic hot-spot generation was also showcased. The best performing YOLOv5 Small model processes images in 168 ms on average during inference, making it a good candidate for real-time operation.

Soon, the integration of the model into the MARTe real-time environment [17] will be done. This way, enabling us to deploy the model in the upcoming OP2 operational campaign and test its performance in real operational conditions.

References

1. Beidler, C.; Grieger, G.; Herrnegger, F.; Harmeyer, E.; Kisslinger, J.; Lotz, W.; Maassberg, H.; Merkel, P.; Nührenberg, J.; Rau, F.; et al. Physics and Engineering Design for Wendelstein VII-X. *Fusion Technol.* **1990**, *17*, 148–168. [CrossRef]
2. Pedersen, T.S.; König, R.; Krychowiak, M.; Jakubowski, M.; Baldzuhn, J.; Bozhenkov, S.; Fuchert, G.; Langenberg, A.; Niemann, H.; Zhang, D.; et al. First results from divertor operation in Wendelstein 7-X. *Plasma Phys. Control. Fusion* **2019**, *61*, 014035. [CrossRef]
3. Klinger, T.; Alonso, A.; Bozhenkov, S.; Burhenn, R.; Dinklage, A.; Fuchert, G.; Geiger, J.; Grulke, O.; Langenberg, A.; Hirsch, M.; et al. Performance and properties of the first plasmas of Wendelstein 7-X. *Plasma Phys. Control. Fusion* **2017**, *59*, 014018. [CrossRef]
4. Klinger, T.; Andreeva, T.; Bozhenkov, S.; Brandt, C.; Burhenn, R.; Buttenschön, B.; Fuchert, G.; Geiger, B.; Grulke, O.; Laqua, H.P.; et al. Overview of first Wendelstein 7-X high performance operation. *Nucl. Fusion* **2019**, *59*, 112004. [CrossRef]
5. Pedersen, T.S.; Abramovic, I.; Agostinetti, P.; Agredano Torres, M.; Äkäslompolo, S.; Alcuson Belloso, J.; Aleynikov, P.; Aleynikova, K.; Alhashimi, M.; Ali, A.; et al. Experimental confirmation of efficient island divertor operation and successful neoclassical transport optimization. *Nucl. Fusion* **2022**, *62*, 042022. [CrossRef]
6. Puig Sitjes, A.; Jakubowski, M.; Naujoks, D.; Gao, Y.; Drewelow, P.; Niemann, H.; Fellinger, J.; Moncada, V.; Pisano, F.; Belafdil, C.; et al. Real-Time Detection of Overloads on the Plasma-Facing Components of Wendelstein 7-X. *Appl. Sci.* **2021**, *11*, 11969. [CrossRef]
7. Degrave, J.; Felici, F.; Buchli, J.; Neunert, M.; Tracey, B.; Carpanese, F.; Ewalds, T.; Hafner, R.; Abdolmaleki, A.; de las Casas, D.; et al. Magnetic control of tokamak plasmas through deep reinforcement learning. *Nature* **2022**, *602*, 414–419. [CrossRef] [PubMed]
8. Merlo, A.; Böckenhoff, D.; Schilling, J.; Höfel, U.; Kwak, S.; Svensson, J.; Pavone, A.; Lazerson, S.A.; Pedersen, T.S. Proof of concept of a fast surrogate model of the VMEC code via neural networks in Wendelstein 7-X scenarios. *Nucl. Fusion* **2021**, *61*, 096039. [CrossRef]
9. Dong, G.; Wei, X.; Bao, J.; Brochard, G.; Lin, Z.; Tang, W. Deep learning based surrogate models for first-principles global simulations of fusion plasmas. *Nucl. Fusion* **2021**, *61*, 126061. [CrossRef]
10. Szűcs, M.; Szepesi, T.; Biedermann, C.; Cseh, G.; Jakubowski, M.; Kocsis, G.; König, R.; Krause, M.; Perseo, V.; Sitjes, A.P.; et al. Detecting Plasma Detachment in the Wendelstein 7-X Stellarator Using Machine Learning. *Appl. Sci.* **2022**, *12*, 269. [CrossRef]
11. Aymerich, E.; Sias, G.; Pisano, F.; Cannas, B.; Carcangiu, S.; Sozzi, C.; Stuart, C.; Carvalho, P.J.; Fanni, A. and JET Contributors. Disruption prediction at JET through deep convolutional neural networks using spatiotemporal information from plasma profiles. *Nucl. Fusion* **2022**, *62*, 066005. [CrossRef]
12. Jalalvand, A.; Abbate, J.; Conlin, R.; Verdoolaege, G.; Kolemen, E. Real-Time and Adaptive Reservoir Computing with Application to Profile Prediction in Fusion Plasma. *IEEE Trans. Neural Netw. Learn. Syst.* **2022**, *33*, 2630–2641. [CrossRef] [PubMed]
13. Kocsis, G.; Baross, T.; Biedermann, C.; Bodnár, G.; Cseh, G.; Ilkei, T.; König, R.; Otte, M.; Szabolics, T.; Szepesi, T.; et al. Overview video diagnostics for the W7-X stellarator. *Fus. Eng. Des.* **2015**, *808*, 96–97. [CrossRef]

14. Zoletnik, S.; Szabolics, T.; Kocsis, G.; Szepesi, T.; Dunai, D. EDICAM (Event Detection Intelligent Camera). *Fus. Eng. Des.* **2013**, *88*, 1405. [CrossRef]
15. Spolladore, L. On the detection of MARFE with visible cameras for disruption prevention. In Proceedings of the Symposium on Fusion Technology, Dubrovnik, Croatia, 18–23 September 2022.
16. Available online: https://www.github.com/ultralytics/yolov5 (accessed on 12 December 2022).
17. Cseh, G. Integrating EDICAM into the MARTe framework. In Proceedings of the Symposium on Fusion Technology, Dubrovnik, Croatia, 18–23 September 2022.